# ON THE INTERACTION BETWEEN A FORWARD-FACING STEP AND TURBULENT BOUNDARY LAYER


**Hannu Eloranta, Pentti Saarenrinne**
Energy and Process Engineering
Tampere University of Technology
P.O. Box 589, 33101 Tampere, FINLAND
hannu.eloranta@tut.fi

**Tsun-Ya Hsu, Timothy Wei**
Rutgers - The State University of New Jersey
Department of Mechanical and Aerospace Engineering
98 Brett Road Piscataway, New Jersey, 08854 – 8085, USA



## ABSTRACT

In this paper the flow around a forward-facing step in a plain channel is studied experimentally using particle image velocimetry and flow visualization. The area of interest lies just upstream of the forward-facing step, particularly in the boundary layer growing on the channel wall opposite to the step. The development of initially turbulent boundary layer under the acceleration generated by the step is assessed by studying both time-mean statistics and instantaneous flow fields. Results show that even though the acceleration parameter $K$ exceeds the critical level of $3.0\times10^{-6}$, the flow statistics do not reach the characteristics of a quasi-laminar state. However, a remarkable decrease of turbulence activity inside the boundary layer is observed. Besides the mean-flow acceleration, the appearance of other modes of interaction between the step shear layer and the boundary layer is also assessed. Conditional averaging and flow visualization are used to discover if strong instabilities in the shear layer can influence the bottom wall boundary layer. In the region covered by the present measurements, any indication of direct interaction between the step shear layer and the boundary layer flow structures cannot be observed.


## INTRODUCTION

A plane nozzle is used in an industrial application to produce a free-surface jet. In this paper, the flow inside the nozzle is studied by reproducing the fundamental fluid dynamics in a very simplified geometry. The geometry of interest is essentially a plain channel with one-sided forward-facing step (FFS) at the channel exit. To put another way, the case to be studied is an asymmetrical 2D-contraction. Figure 1 illustrates the time-mean flow pattern close to the FFS by means of the streamlines. The flow is from left to right. In the present setup the development of the jet downstream of the nozzle exit cannot be studied. Experiments are performed only inside the nozzle to understand the role of flow instabilities and large-scale flow structures to the jet quality.

Previous work on this subject (Hsu, 2002) has focused on the instabilities generated by the step. From that work, which will be summarized in the following, it is evident that large-scale instabilities originate from the step. Now, those instabilities are reflected to the ones found on the opposite wall boundary layer. Their relative strength and possible interactions are assessed. Measurements are performed by particle image velocimetry (PIV). In addition, flow visualization is used to illustrate the flow structures.

The FFS generates an intense streamwise acceleration and streamline curvature as the flow passes by the blockage. The effects of acceleration to a turbulent boundary layer have been studied extensively in the literature. Experiments both with constant streamwise pressure gradient and spatially varying acceleration have been performed. Usually the acceleration is quantified by a non-dimensional acceleration parameter $K$, which is defined as:

$$K=\frac{\nu}{U_e^2}\frac{dU_e}{dx} \qquad (1)$$

, where $\nu$ is the kinematic viscosity and $U_e$ the free-stream velocity.

Even though it is obvious that this parameter cannot solely characterize the development of a boundary layer under acceleration, it seems that the value of $K > 3.0\times10^{-6}$ is a critical

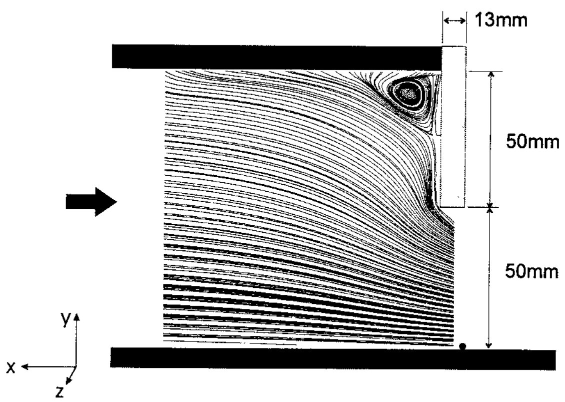


Figure 1. Forward-facing step in the channel and the mean flow streamlines.

requirement for the relaminarisation to take place. Numerous studies have been performed, but unambiguous definition or parameter to mark the onset of relaminarisation has not been established. This is predominantly due to the gradual changes and somewhat overlapping boundaries between different phases in the laminarisation.

Especially in the past, much of the work concentrating on the boundary layers under favorable pressure gradient have been focused on the characteristics of the mean flow. Thus, these aspects, such as the streamwise development of momentum thickness, shape factor, turbulence intensity and boundary layer thickness, are pretty well established. Reviews by Narasimha & Screenivasan (1979) and Screenivasan (1982) survey the basic concepts and the development of relaminarisation extensively. Experiments using spatially varying acceleration are for example those of Escudier et al. (1998) and Blackwelder & Kovasznay (1972).

Also the development of computational methods during the last two decades has created important simulated data on the subject. Spalart (1986) using direct numerical simulation (DNS) studied three levels of acceleration in a sink-flow. Piomelli et al. (2000) used LES to explain the dynamics of flow structures in a spatially accelerating boundary layer.

The main conclusion of all these studies is that a strong enough acceleration can revert initially turbulent boundary layer into a quasi-laminar state, which resembles a laminar boundary layer. The change takes place gradually in a process where relative turbulence intensity decreases especially in the mid-boundary layer and low-frequency patches appear to the flow. During the relaminarization energy shifts to the larger scales. The streaks became highly elongated in the streamwise direction. Eddies decrease in number and are more oriented in the streamwise direction. Fewer ejections into the outer layer are also observed.

The work of Hsu showed that besides creating an intense acceleration, the FFS is a remarkable source of instability. In the time-mean frame, a spanwise vortex is developed in the corner of the top-wall and the blockage. Examination of instantaneous velocity fields reveals that this vortex is neither fixed in location nor constant in size. Occasionally more than one spanwise vortex appears in the corner. Instantaneous velocity fields measured from the end view (i.e. parallel to the plane of the FFS wall) show that also streamwise vortices are generated upstream of the FFS. These vortices first appear in the upstream close to the top-wall. To the down-stream direction they move away from the top-wall and pass under the edge of the FFS. The origin of these streamwise vortices appears to be strong shear and embedded instability mechanisms.

## EXPERIMENTAL SETUP

The experiments are carried out in a free-surface water tunnel facility. The tunnel provides controlled and disturbance-free flow to the test section. A 2D-contraction is placed in the test section to accommodate the nozzle model. Details of the contraction and the water tunnel facility are provided in the work of Hsu.

Velocity data is acquired in three planes normal to each other. The imaging system consists of a Kodak Megaplus ES1.0 (1.0 Mpix) dual-frame camera with Nikkor lenses (50mm f/1.8 or 105mm f/2.8), New Wave Gemini Nd:YAG laser, a Standford DG535 pulse generator, a PC with frame grabber and Kodak software to store the images. Silver-coated hollow glass spheres with a nominal diameter of 10μm are used as tracer particles. The most important dimensions of the channel is indicated in the figure 1. The total length of the plane channel is 750mm and the transverse dimension (in the $z$-direction) is 550mm. The coordinate system is also defined in the figure 1. The origin is located on the bottom wall right under the downstream edge of the FFS, marked by a dot. From this point, the streamwise coordinate $x$ runs positive to the upstream direction. Nevertheless, velocity is defined to be positive in the streamwise direction (marked by the arrow). Position labelled by '$x$=50mm' stands for a location 50mm upstream of the step.

Flow visualization is performed in $y$-$z$ –plane. Fluorescent dye is injected into the flow trough slits machined to the top and bottom walls. The slits are 150mm wide and placed in the middle of the channel in the $z$-direction. On the bottom wall the slit is at the position $x$=100mm and on the top wall at $x$=50mm. Nd:YAG –laser with laser sheet optics is used to charge the dye and the light emitted is detected with the Kodak Megaplus camera. The setup used for flow visualization is essentially the same as that used for PIV.

## RESULTS

First a short description of the statistics measured on the bottom wall is presented. This done to characterize the state of the boundary layer and its' development under acceleration. More details can be found in Eloranta (2002).

The streamwise distribution of the acceleration parameter $K$ is presented in figure 2. The maximum of $K$ achieved around $x$=20mm is $6.75 \times 10^{-6}$. After this peak, the acceleration parameter starts to decrease. Figure 2 also shows the development of the Reynolds number based on the boundary layer momentum thickness, $Re_\theta$. Reynolds number diminishes at a constant rate between $x$=85mm and $x$=20mm, after which the drop slows down. $Re_\theta$ remains at around 450 as the flow exits the channel.

The mean-velocity profiles at the downstream positions are strongly distorted by the presence of the FFS. The maximum velocity is located on the edge of the boundary layer, which suggests that the influence of the FFS penetrates close to the opposite wall. Plotted with the real distance from the wall on the $y$-axis, these profiles show that the boundary layer thickness decreases towards the FFS (not shown here). Nevertheless, the same velocity data plotted with the streamfunction on the $y$-axis, as presented in figure 3, indicates that the boundary layer thickness remains almost constant. In other words, the edge of the boundary layer coincides with a streamline and the streamlines move closer to the wall. In contrast to this, both Blackwelder & Kovasznay and Escudier et al. observed that the streamfunction on the edge of the boundary layer decreases to the downstream direction. In the most downstream profiles a distinct kink appears in the near-wall region.

The development of turbulence is depicted by plotting streamwise profiles for $U_{x,rms}$ and $U_{y,rms}$. This is done by choosing three streamlines, along which the intensities are followed. The streamline at $\psi$=15000 is on the edge of the

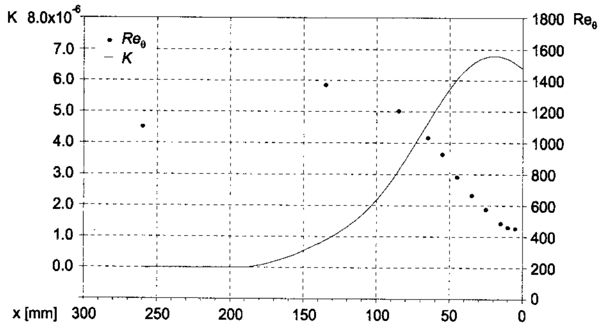


Figure 2. Streamwise development of the acceleration parameter $K$ and $Re_\theta$.

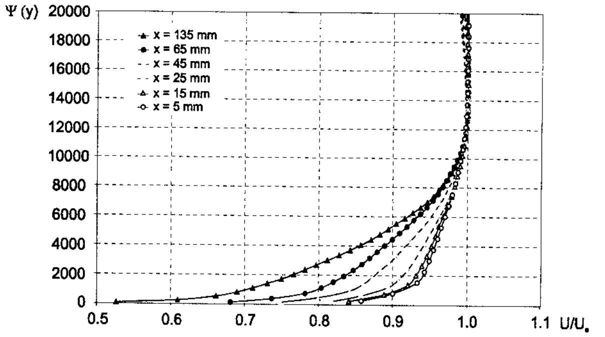


Figure 3. Development of the wall-normal velocity profiles under acceleration.

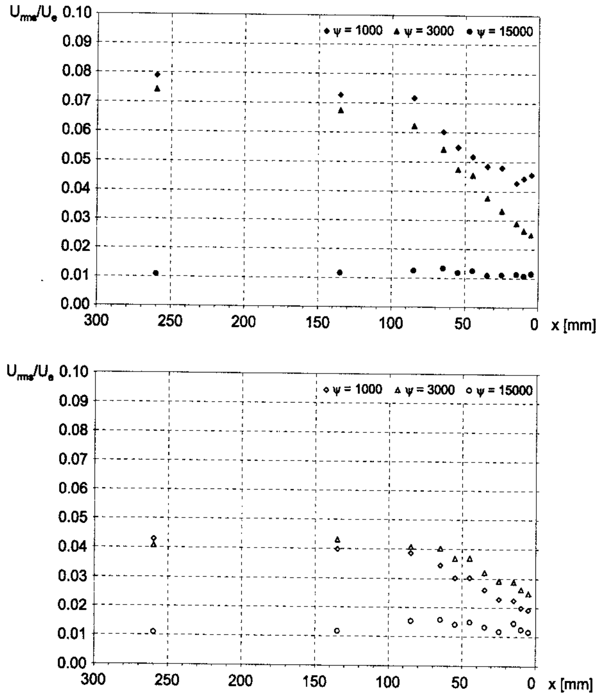


Figure 4. Streamwise profiles of turbulence intensity along three streamlines. Black symbols in the upper chart denote x-component and white in the lower one y-component.

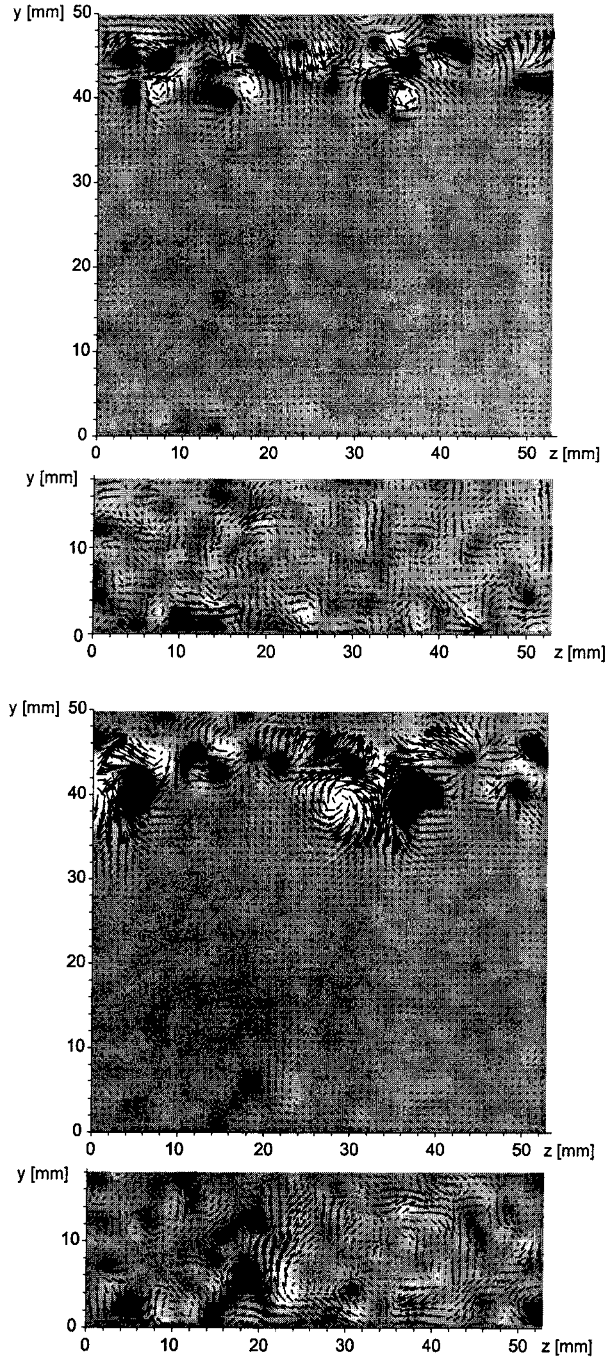


Figure 5. Two examples of instantaneous flow fields in the $y$-$z$-plane just under the step. Small windows represent the lower part of the field re-scaled to adduce the boundary layer structures.

boundary layer. Development in the mid-layer is examined at the level $\psi$=3000. Even though the resolution close to the wall is only moderate, $\psi$=1000 is chosen to represent the near-wall area. In figure 4, the velocity fluctuation rms-values are normalized by $U_e$, i.e. the local free-stream velocity. Outside the boundary layer the turbulence intensity remains essentially constant, but in the mid-boundary layer the turbulence intensity decreases significantly. The peak of $U_{x,rms}$ close to the wall cannot be accurately resolved due to the extremely

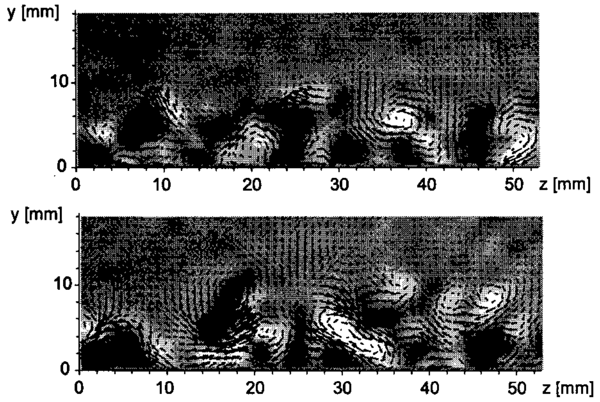


Figure 6. Two examples of instantaneous flow fields in the y-z-plane measured in the upstream turbulent boundary layer.

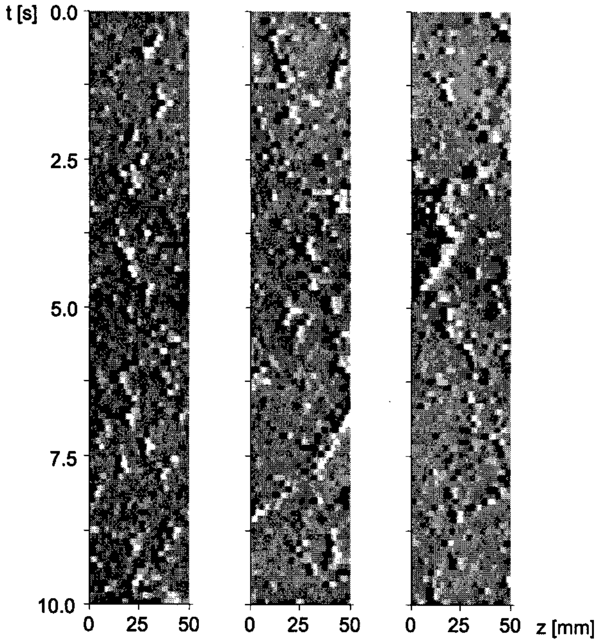


Figure 7. Three vorticity time-sequences in the step shear layer.

small boundary layer thickness. Over most of the positions, the trend of decaying turbulence intensity is obvious at least down to $\psi$=1000. However, close to the position $x$=0mm the decrease is slowed down or even halted. Actually, over the last few downstream positions, the level of $U_{x,rms}$ is increasing in absolute terms, i.e. without scaling by $U_e$. These results are in accordance with studies of Escudier et al. and Blackwelder & Kovasznay.

Next, two instantaneous flow fields in the *y-z* – plane are presented. Both fields are measured just under the downstream edge of the step. The uppermost frame in figure 5 covers the entire channel height under the step. The second small frame is cropped from the wall-region of the first one and re-scaled. This is done to visualize the boundary layer structures, which are almost an order of magnitude weaker than those present in the step shear layer. The contours on the background represent streamwise vorticity $\omega_x$ and the vectors velocity fluctuations according to the Reynolds decomposition. In the first frame the scale of vorticity is set to ±3001/s and in the second frame to ±100 1/s. Below these two, another pair of frames presents another instantaneous flow field.

The first pair shows three vortex pairs beneath the edge of the step. On the bottom wall, the flow field appears to be quite smooth, which is interpreted as a consequence of relaminarisation. The second pair portrays two large-scale vortex pairs in the step-shear layer and a rather weak vortex pair in the boundary layer. The small frames can be compared with figure 6, which shows two instantaneous fields measured in the upstream at $x$=250mm. This location is in the region, where acceleration in not acting yet and the boundary layer can be considered as fully turbulent. Again the contours on the background represent streamwise vorticity and the scale is ±100 1/s. In both frames streamwise vortices fill the whole span across the window. They are also stronger than in the downstream position. It can be stated (based on the examination of hundreds of frames) that the number of streamwise vortices in the boundary layer decreases significantly under acceleration. This observation specifies the results in figure 4 showing reduced turbulence activity in the downstream positions.

To address the questions of the vortex generation and their time-scales in the step shear layer, PIV-data is used to produce a time-sequence of vorticity. This is performed by extracting one row of data in each velocity field and combining consecutive rows into a new plot with $z$-location on the x-

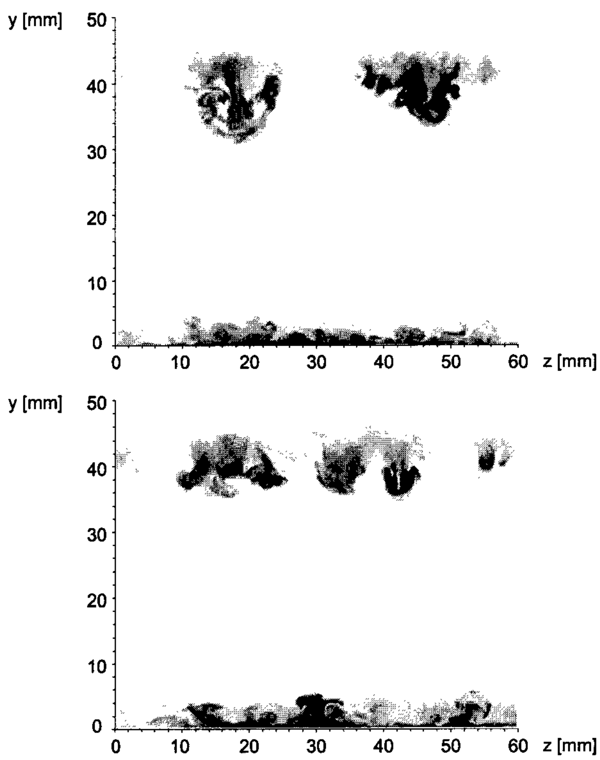


Figure 8. Two frames from the flow visualizations just under the step in the *y-z*-plane

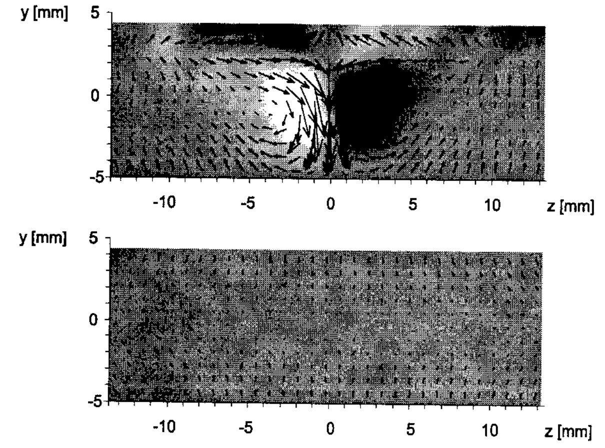


Figure 9. Conditionally averaged flow patterns related to a strong negative velocity under the step.

axis and time on the *y*-axis. The camera frequency is only 10Hz, but since strong vortices remain at fixed positions over the period of several frames, estimation of the scale of the largest vortices can be deduced. Figure 7 presents three this kind of vorticity time-sequences. Time resolution is 0.1s and by using the mean convective velocity of 2.0m/s this corresponds to a spatial resolution of 0.2m. Even though it is not clear if vorticity that remains at a fixed location over several frames indicates a single vortex pair or a sequence of individual vortex pairs, which are triggered and born one after another, the vorticity forms extremely large-scale structures. In the figures the spanwise wandering of the vortices seems to be remarkable, but it has to be emphasized that it is only in the order of 20mm. On the other hand, the time-scale of the structures may be as large as 10 frames (1 second), which corresponds to 2m in length. Similar analysis in the boundary layer does not indicate any large-scale vortices.

Figure 8 presents two frames from the flow visualizations performed in the *y-z* –plane just under the step. The same phenomena as in the figure 5 can be observed here. Vortex pairs in the step shear layer are visible in both frames. One has to be careful on making conclusions from the boundary layer structures, since the dye as a passive scalar tends to depict the history of the flow rather than the actual vorticity. The dye was injected in the upstream to a turbulent boundary layer and what is observed at *x*=0mm may result from the vorticity prior to the onset of relaminarisation. Partly relaminarized boundary layer beneath the step does not have the vorticity to transport the dye anymore.

One of the important questions that were originally motivating the present study was, what kind of interaction there is between the step and bottom wall boundary layer. The principal mode of interaction is naturally the acceleration due to the sudden contraction, which was explored in terms of the time-mean turbulence quantities. In addition to the mean flow pattern other modes of interaction are conceivable. The appearance of strong vortex pair close to the step might create a disturbance, which would affect the flow on the bottom wall. To study if this kind of mechanism could be found in the present case, data in the *z-y* –plane was analysed carefully. The flow visualizations or PIV-data do not indicate any direct momentum transfer between the layers. Even though the flow structures from the step shear layer occasionally extend to the half way between the step and bottom wall, actual pairing of the vortices in these layers cannot be observed. This may happen later in the downstream, which is out of the measurement region in the present study.

Another strategy is developed to look for possible interaction around the position *x*=0mm. Conditional averaging is utilized to reveal if the occurrence of strong vortex pair in the shear layer induces something typical on the opposite wall. In each instantaneous field the magnitude of wall-normal velocity component was threshold along a spanwise line just under the step. Strong negative values signify down wash of fluid towards the bottom wall, which typically occurs due to streamwise vortex pairs. Using strong negative wall-normal velocity as the condition for averaging, a mean flow pattern presented on top the figure 9 is achieved. This flow field is established by cropping and storing a window with a size of 25x10mm$^2$ centred to the location of maximum down wash and averaging over the collected samples. Every time a sample is cropped, the flow pattern on the opposite wall is stored too. This way the conditional average- and rms-fields for the boundary layer can be established. Conditional average of the boundary layer flow pattern is presented also in the figure 9. This analysis do not bring forward any secondary flow structure or even increased turbulence energy compared to randomly sampled locations. To further verify this result some sequences, in which streamwise vortex pair remains at a constant location over several frames are analysed by visually inspecting the vorticity fields close to the bottom wall. The results from this study do not either reveal any characteristic structure related to long streamwise vortex pairs on the opposite wall.

## CONLUSIONS

In this paper a complex turbulent flow appearing in a nozzle used for an industrial application is studied by isolating the fundamental fluid dynamics to a very elementary flow configuration. The geometry of interest is essentially a 2D-channel with one-sided forward-facing step on the upper wall. The results presented in this report show that the primary mode of interaction between the step and the boundary layer results from the mean acceleration field. Strong favourable pressure gradient tends to relaminarize turbulent boundary layer. This trend is obvious in the present case, even if complete relaminarisation cannot be observed. However, remarkable alterations in the structure of turbulence inside the boundary layer are observed. At the edge of the boundary layer the velocity fluctuations are quite isotropic in the upstream. This is naturally not the case inside the boundary layer. But as a result of the acceleration, the difference between $U_{x,rms}$ and $U_{y,rms}$ also in the mid-boundary layer decreases remarkably and just under the step they are equal in magnitude. In contrast, very close to the wall increase of $U_{x,rms}$ enhances unisotropy further. Compared to the boundary layer turbulence, the structures evolving in the step shear layer are an order of magnitude stronger. Direct impact of these structures to the relaminarizing boundary layer is studied by flow visualization and conditional averaging of the PIV-data. However, no indication of direct interaction between these vorticity layers is observed.

## REFERENCES


Blackwelder, R.F. & Kovasznay, L.S.G 1972, Large-scale motion of a turbulent boundary layer during relaminarization, *J. Fluid Mech.*, vol 53. pp. 61-83.

Eloranta, H., Hsu, T.Y., Wei. T. & Saarenrinne P. 2002, A PIV study on the interaction between a forward-facing step and turbulent boundary layer. Presented in Application of Laser techniques to Fluid Mechanics, July 10th-13th, Lisbon, Portugal.

Escudier, M.P., Abdel-Hameed, A., Johnson, M.W. and Sutcliffe, C.J. 1998, Laminarisation and re-transition of a turbulent boundary layer subjected to favourable pressure gradient. *Exp. in Fluids*, 25, pp. 491-502.

Hsu, T.Y. 2002, Hydrodynamics of Paper Making: Streamwise Vortices Generated in Upstream of a 2-D Jet Nozzle, Doctoral Thesis, Rutgers; The State University of New Jersey, USA.

Narasimha, R. & Screenivansan, K.R. 1979, Relaminarization of fluid flows. *Advances in applied mechanics*, vol 19, pp. 221-309.

Piomelli, U., Balaras, E., & Pascarelli, A. 2000, Turbulent structures in accelerating boundary layers, *Journal of Turbulence,* http://jot.iop.org/, 1/2000.

Screenivasan K.R. 1982, Laminarescent, relaminarizing and retransitional flows. *Acta Mechanica*, 44, pp. 1-48.

Spalart, P.R. 1986, Numerical study of sink-flow boundary layers, *J. Fluid Mech.*, vol. 172, pp. 307-328.

Talamelli, A., Fornaciari, N., Westin, K.J.A. and Alfredson, P.H. 2002, Experimental investigation of streaky structures in a relaminarizing boundary layer, *Journal of Turbulence*, http://jot.iop.org/, 3/2002, 018, 13 p.